UCRL-JC-130495
PREPRINT

HPGe Compton Suppression Using Pulse Shape Analysis

G. J. Schmid, D. Beckedahl, J. J. Blair, J. E. Kammeraad

This paper was prepared for submittal to the
1998 Symposium on Radiation Measurements and Applications
Ann Arbor, MI
May 11-14, 1998

April 15, 1998

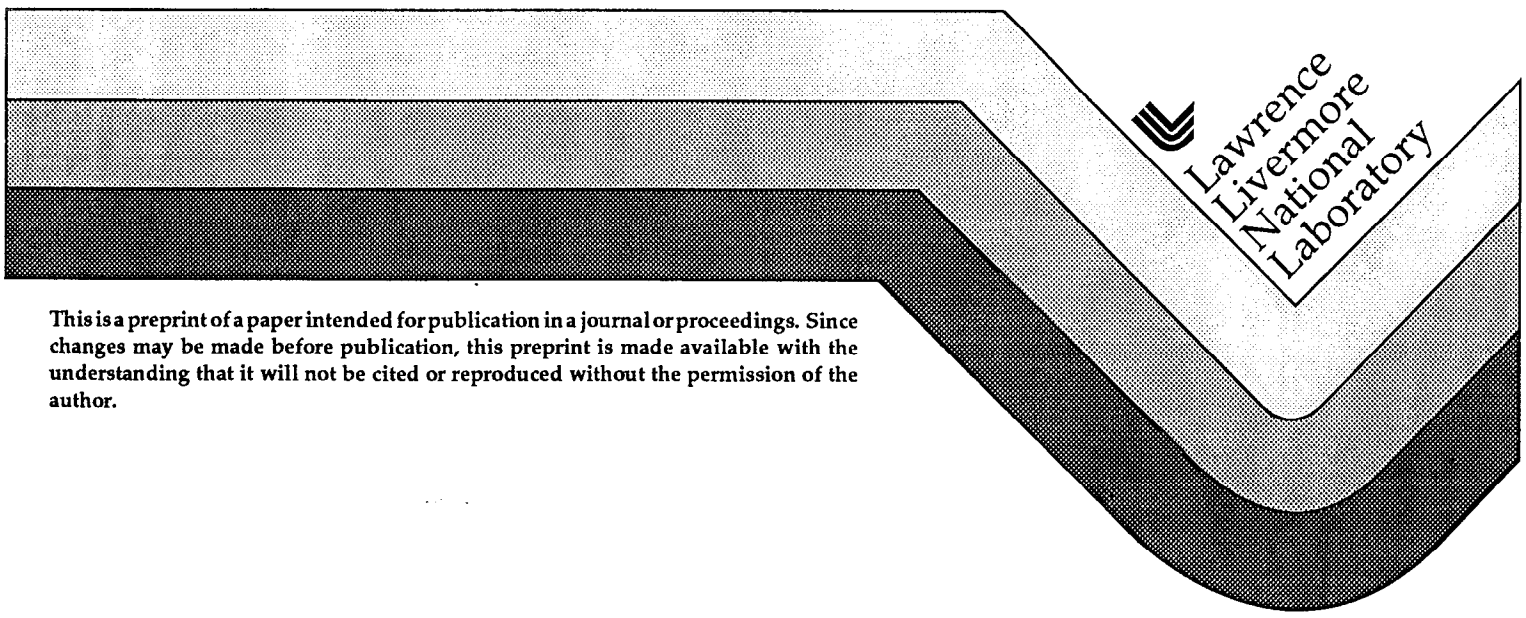

HPGe Compton suppression using pulse shape analysis

G.J. Schmid[a], D. Beckedahl[a], J.J. Blair[b], J.E. Kammeraad[a]

[a]Lawrence Livermore National Laboratory
University of California, Livermore, CA 94550

[b]Bechtel Nevada
North Las Vegas, NV 89130-4134

Abstract

We present a new technique for High Purity Germanium (HPGe) Compton suppression using pulse shape analysis (PSA). The novel aspect of our approach involves a complete unfolding of the charge pulse shape into a discrete sum of component γ-ray interactions. Using the energy and position information obtained from such an unfolding, an algorithm is then applied which favorably rejects Compton escape events. The advantage of the current PSA approach, as compared with other recent approaches, is the potential to reject not only single-site escape events, but also multiple-site escape events. Here we discuss the details of our algorithm, and present experimental results from a real-time implementation on a 5 cm x 5 cm HPGe. An experimental comparison with a standard BGO suppressor is shown. We also discuss the possible improvements to the current PSA approach that could be obtained if the HPGe could be highly segmented on the outer contact.

This work was performed under the auspices of the U.S. Department of Energy by Lawrence Livermore National Laboratory under contract No. W-7405-Eng-48.

HPGe Compton suppression using pulse shape analysis

G.J. Schmid[a], D. Beckedahl[a], J.J. Blair[b], J.E. Kammeraad[a]

[a]Lawrence Livermore National Laboratory
University of California, Livermore, CA 94550

[b]Bechtel Nevada
North Las Vegas, NV 89130-4134

Abstract

We present a new technique for High Purity Germanium (HPGe) Compton suppression using pulse shape analysis (PSA). The novel aspect of our approach involves a complete unfolding of the charge pulse shape into a discrete sum of component γ-ray interactions. Using the energy and position information obtained from such an unfolding, an algorithm is then applied which favorably rejects Compton escape events. The advantage of the current PSA approach, as compared with other recent approaches, is the potential to reject not only single-site escape events, but also multiple-site escape events. Here we discuss the details of our algorithm, and present experimental results from a real-time implementation on a 5 cm x 5 cm HPGe. An experimental comparison with a standard BGO suppressor is shown. We also discuss the possible improvements to the current PSA approach that could be obtained if the HPGe could be highly segmented on the outer contact.

1. Introduction

To reject Compton background in γ-ray spectroscopic measurements, one typically surrounds the primary detector (e.g. a Ge crystal) with a secondary detector (the "suppressor") operated in anti-coincidence mode. Because of its high stopping power, Bismuth Germanate (BGO) is usually chosen as a suppressor. Unfortunately, the large size, weight, and cost of a BGO crystal can often overwhelm any possible benefits, especially for measurements performed in the field. For this reason (and others), a Compton suppression technique based only on details of the charge pulse shape seems attractive.

Recent efforts to apply Ge detector pulse shape analysis (PSA) to Compton suppression [1,2,3,4,5] have focused on general characteristics of the charge pulse shape (e.g. rise-time, single-site shape vs. multiple site-shape). We present here a more fundamental approach based on a complete unfolding of the charge pulse shape into a sum of component pulse shapes associated with each γ-ray interaction. Using the acquired energy and position information, we can then apply an algorithm which allows us to discriminate between full energy deposition events, and escape events (γ rays which deposit less than their full energy in the crystal). The algorithm is chosen so as to allow for discrimination on both single-site and multiple-site escape events. This differs from the algorithms of [1,4] which were designed to reject only single-site events. Below, we present the details of our algorithm along with experimental results from a real time implementation on a 5cm x 5cm High Purity Germanium (HPGe) detector.

2. Compton suppression procedure

2.1 HPGe detector

Our HPGe detector is a 5 cm x 5 cm closed-ended coaxial (1 cm diameter hole). Its measured efficiency is 20% at 1.332 MeV as compared with a 3"x3" NaI. Although a planar region of ~1cm in depth exists at the front face, our algorithm operates only in the

pure coaxial part. In effect, we treat the planar region as a dead layer, throwing out events which occur there, and accepting only those events which occur primarily in the coaxial region (as described in the following section).

2.2 Charge pulse shape

For γ rays in the energy range 150 keV to 10 MeV, Compton scattering is the most probable interaction in Ge, and a full absorption event typically involves a multiple Compton path ending in photoabsorption. For the 5 cm x 5cm HPGe crystal which is of interest in this study, a 1 MeV γ ray which deposits all of its energy will usually Compton scatter 2-4 times before photoabsorbing. For the pure coaxial region of the HPGe, the charge pulse shape for a given interaction is dependent only on the radial position of that interaction [6]. The charge pulse shape which is viewed at the HPGe preamplifier is then a linear sum of the charge pulse shapes produced by each interaction site (with each term weighted by the energy deposited at that site).

Experimentally, we determined the charge pulse shape for a given set of radial bins using a highly collimated beam of γ rays from a ^{137}Cs source. For each event, the pulse shape was digitized at 250 million samples/sec (this actually oversamples the system bandwidth by a factor of five). More explicit details of our set-up will be published [7]. By gating on the Compton edge, a single-site event is made to be highly probable. We further filter out multiple-site events by comparing the measured pulse shapes to calculated pulse shapes using the form given in [6]. In a similar manner, we can discriminate against planar events, which will also have a different shape. The measured charge pulse shape for each radial bin is then treated as a basis function for expansion of an arbitrary pulse shape. The coefficients of this expansion represent the fractional energy deposition in each radial bin. The expansion is actually performed by a least-squares fit. A "steepest descent algorithm" [8] is employed to find a solution in the 10-dimensional coefficient space.

2.3 Maximum fractional energy deposition

For a given γ ray event, two sets of coefficients are obtained. One set is based on 10 radial zones with Δr (the width) = 2mm. These radial zones are rings with cross sectional area $2\pi r(\Delta r)$, and they start at the inner contact (r=6mm is the radial center of the 1st zone) and end at the outer contact (r=24mm is the radial center of the last zone). The second set of zones is also 2mm in width, but is shifted by 1mm with respect to the first set of zones. Using the two sets of coefficients derived from the two different sets of zones, we can then determine the maximum fractional energy deposition, E*, that is possible in an arbitrary zone of area $2\pi r(\Delta r)$, with Δr=2mm.

2.4 Rejection criteria

Our rejection algorithm operates as follows: all events with E* less than a certain cutoff, as defined by the function $f(E_{dep})$, are accepted. All others are rejected. The cutoff function is defined as follows:

$$f(E_{dep}) = \frac{2.0}{2.0 + \frac{511.0}{E_{dep}}} \qquad \text{for } E_{dep} > 372 \text{ keV} \tag{1}$$

$$f(E_{dep}) = \frac{\alpha}{E_{dep}} \qquad \text{for } E_{dep} < 372 \text{ keV}$$

where E_{dep} is the total energy deposited by the γ ray (in keV), and α is a constant empirically determined to be 220 keV.

The form of (1) is based on the energy deposition characteristics of γ-rays which fully absorb in the HPGe. At higher energies (E_γ>372 keV) a Compton backscatter will

typically provide the highest energy interaction point, and thus we accept only events whereby E* is less than $f(E_{dep})=E_c(E_{dep})/E_{dep}$, where E_c is the Compton edge as calculated assuming that $E_{dep}=E_\gamma$. At lower energies ($E_\gamma<372$ keV), the photoabsorption event at the end of the path becomes the dominant interaction point, and thus we only accept events whereby E* is less than $f(E_{dep})=\alpha/E_{dep}$, where α is the energy deposited by a typical photoabsorption interaction. Studies using a GEANT [9] Monte Carlo simulation have determined α to be 220 keV for a medium energy (500 keV) γ ray incident on our HPGe crystal. With this value of α inserted into the low energy form for $f(E_{dep})$, it is seen that the low energy and high energy forms for $f(E_{dep})$ cross at 372 keV.

Since the low energy form for $f(E_{dep})$ crosses 1.0 at 220 keV, this is the energy at which the algorithm turns off (i.e. no events rejected below this energy). Conversely, above 220 keV the algorithm is always less than 1.0, and this indicates that single hit events (which, by definition, give $f(E_{dep})=1$) are always rejected when the algorithm is on.

2.5 Multiple-site escapes

As mentioned above, all single-site events are rejected. This will include the majority of escapes. However, a significant fraction of escape events are multiple-site in nature. It is of interest, therefore, to note that the above algorithm is also designed to reject a certain percentage of these multiple-site escapes. To demonstrate this principle, Figure 1 shows a scatter-plot displaying the results of a Monte Carlo simulation for γ rays incident on the front face of our HPGe detector. The energies of the γ rays are randomly chosen from the energy range 0.3-1.3 MeV. The quantities plotted are E_{ffrac}, the maximum fraction energy deposition for a single interaction, and $x(E_{dep})=1+256/E_{dep}$, where E_{dep} is in keV. Full energy absorption events are indicated by the filled circles, while escape events are indicated by open circles. Only multiple-site events are shown. The cut predicted by (1) above, which appears on this plot as $1/E_{frac}$ is shown on this plot by the solid line. Since all

events above the line will be rejected, it is clear from this simulation that discrimination of multiple-site escapes is possible.

3. Experimental results

Figure 2 shows the experimental set-up used. A ^{152}Eu source was placed 25 cm on-axis from the front face of our HPGe detector. The source strength was such that the overall count rate in the HPGe was ~1 kHz. Data was acquired both with the HPGe alone (BGO annulus removed) for testing the current PSA algorithm, and also with the BGO annulus [10] in place, for purpose of comparison with the standard BGO rejection technique. In both cases, data was acquired in real time. In data analysis, which was performed off-line at a later time, peak areas from the ^{152}Eu spectra (both PSA and BGO discriminated) were extracted by comparing on-peak and off-peak sum windows.

In a background dominated environment, the quantity of interest is the peak height as compared with the fluctuation of the local background. If the on-peak sum window is denoted as P, and the off-peak sum window is denoted as B (i.e. background), then:

$$S = \frac{N}{\sqrt{B}}, \tag{2}$$

where N=P-B, and S is the peak sensitivity. The effectiveness (ε) of a given suppression technique is then given by the ratio of S for the suppressed (S') and unsuppressed (S_0) cases. An effectiveness greater than 1 indicates a net gain in spectrum quality.

Figure 3 shows ε for six strong peaks in the ^{152}Eu spectrum. Although the PSA discrimination gives ε greater than 1 for six of the seven peaks, the BGO suppression clearly dominates in all cases.

4. Discussion

4.1 Performance critique

The origin of performance degradation in the PSA rejection technique can be traced to three primary causes:

1. Interaction points that add within a single radial zone (thus simulating a point of higher energy).
2. Interaction points that deposit energy within the planar region.
3. An incorrect solution in the least squares fitting procedure.

In order to better understand the scope of these three effects, a computer simulation of the PSA rejection procedure was undertaken. By taking the output of a GEANT Monte Carlo run (energies and positions of γ ray interactions), and sending it through a virtual data processing system that modeled our actual set up [7], a realistic pulse shape could be simulated for each event. This procedure included the addition of system bandwidth response and white noise (15 keV rms per channel) to each pulse shape. The pulse shape was then digitized and a value of E* extracted.

The simulations show that the primary cause for performance degradation is the addition of interaction points within a zone (#1 above). When this occurs, the extracted E* value will often move from a location below the cut-off (see Figure 1) to a location above the cut-off, and thus reduce the peak detection efficiency. For example, the 964 keV peak in the ^{152}Eu spectrum is predicted to undergo a 30% drop in efficiency due to this effect alone. To eliminate this effect, one could consider increasing the number of radial zones. However, simulations indicate that the interaction points (whose size can approach 1mm due to recoil electrons) will begin to overlap before large gains in performance can be realized. A more promising approach is to separate out the points by their respective depth in the detector. This can be accomplished if the outer contact is highly segmented (section 5).

The second most important effect is loss of peak efficiency due to interactions in the planar region (#2 above). This accounts for the majority of the remaining 20% drop in efficiency that is observed (50% drop overall). The only solution here is to remove the

planar region entirely. However, this could introduce new problems in the form of surface currents.

The third problem (#3 above) is the acquisition of an incorrect solution for the energy deposition in the crystal. Figure 4 shows, from simulation, how the quantity E_{frac} – E* looks for a 1 MeV incident γ ray (E_{frac} being the actual maximum energy fraction, as compared with E* which is the maximum energy fraction derived from the PSA). The events which have been histogrammed in Figure 4 are all well separated (> 2 mm) and substantially energetic (>50 keV). As can be seen from the figure, the effect of the incorrect solution is typically to underpredict E_{frac} by 3-13%, with a 1σ spread of 7-10% about the average deviation. Since the average deviation is downwards, the net effect is to increase the number of escape events which are incorrectly incremented in the spectrum. This will increase the background, but will not substantially effect peak efficiency.

4.2 Rejection of multiple-site escapes

As previously discussed, one of the advantages of the current algorithm is that we attempt to explicitly reject multiple site escapes. In particular, of the 1.0 MeV γ rays that escape from the detector (with source 25 cm away on-axis), 40% are multiple hit escapes. Using the PSA computer simulation discussed above, we find that 60% of the multiple hit escapes, as compared with 70% of the single hit escapes, are rejected by the current PSA algorithm (for 1 MeV incident γ rays).

5. Improvement through segmentation

As discussed in section 4, the primary cause of performance degradation in the PSA technique is the summing of interaction points within a given radial zone. This problem could be largely alleviated by highly segmenting the outer contact of the HPGe. As discussed below, this would allow localization of the interaction points in 3-dimensions (r,ϕ, and z in cylindrical coordinates), and thus points could be better separated.

In this approach, the outer contact of the HPGe is divided into many segments (perhaps as many as 36). By looking at the signals from each segment, one then deduces the hit pattern of the incident γ ray in 3-dimensions. This can be accomplished by solving the Poisson equation, with appropriate boundary conditions, for a grid of points within the HPGe volume. An interaction at a given point will then have a given set of associated pulse shapes on the outer contacts. For multiple interactions, one would then seek to unfold the measured set of pulse shapes into a sum of discrete interaction pulse shape sets.

Although we have not yet completed our study of this approach, we have done GEANT Monte Carlo simulations which indicate that significant gains could be made in PSA Compton rejection over what we have now. In particular, if we assume a 3-dimension position resolution of ~1mm (in cylindrical coordinates, Δr=1mm, $\Delta\phi$=.066 rad, Δz=1mm), the current algorithm is seen to improve in effectiveness by 20% for the 964 keV line in ^{152}Eu . Furthermore, with this degree of position resolution, a new algorithm based on Compton tracking can also be applied. In this algorithm, we examine all possible ordering sequences of the interaction points to find a path which is consistent with the Compton scattering formula. If such a sequence can be found, the γ ray is accepted, otherwise it is rejected. GEANT Monte Carlo simulations indicate that this algorithm, if implemented, could increase the effectiveness by 30% over the current value for the 964 keV line in ^{152}Eu.

6. Conclusion

As shown in figure 3, one can obtain an improvement in spectrum quality using the current PSA rejection technique. However, the total performance as a Compton suppressor is still not competitive with that of a large BGO annulus. Therefore, for a given application, one must decide if the various advantages of the PSA technique outweigh the overall lower performance. Important advantages are:

1. Larger field of view. The current PSA technique allows, in principle, a 4π field of view, while BGO technique sees only γ rays entering the front face.
2. Lower volume. The BGO suppressor increases detector volume by more than an order of magnitude.
3. Lower weight. The BGO suppressor adds ~75 lbs to the total weight.
4. Lower cost. The BGO suppressor [10] was purchased in 1992 for $67,000. It is estimated that the current PSA technique could be fielded for much less.

References

1. B.Philhour, S.E. Boggs, J.H. Primbsch, et al., NIM A403 (1998)136
2. B. Aspacher, A.C. Rester, NIM A338 (1994)511
3. B. Aspacher, A.C. Rester, NIM A338 (1994)516
4. F. Petry, Prog. Part. Nucl. Phys 32 (1994)281
5. A. Del Zoppo, C. Agodi, R. Alba, et al., NIM A334(1993)450
6. Glenn Knoll, Radiation Detection and Measurement, chapter 12, John Wiley & Sons, NY, 1989
7. G.J. Schmid, D. Beckedahl, J.J. Blair, J.E. Kammeraad, To be published
8. W.H. Press, S.A. Teukolsky, W.T. Vettereing, B.P. Flannery, Numerical Recipies in C, Cambridge University Press, 1992
9. R. Brun, F. Bryant, M. Maire, A.C. McPherson, P. Zanarini, GEANT3 users' guide, DD/EE/84-1, CERN 1987
10. BGO suppressor, model 7.75HW9BGO/(8)1.5L-X from BICRON corp., Newbury, Ohio

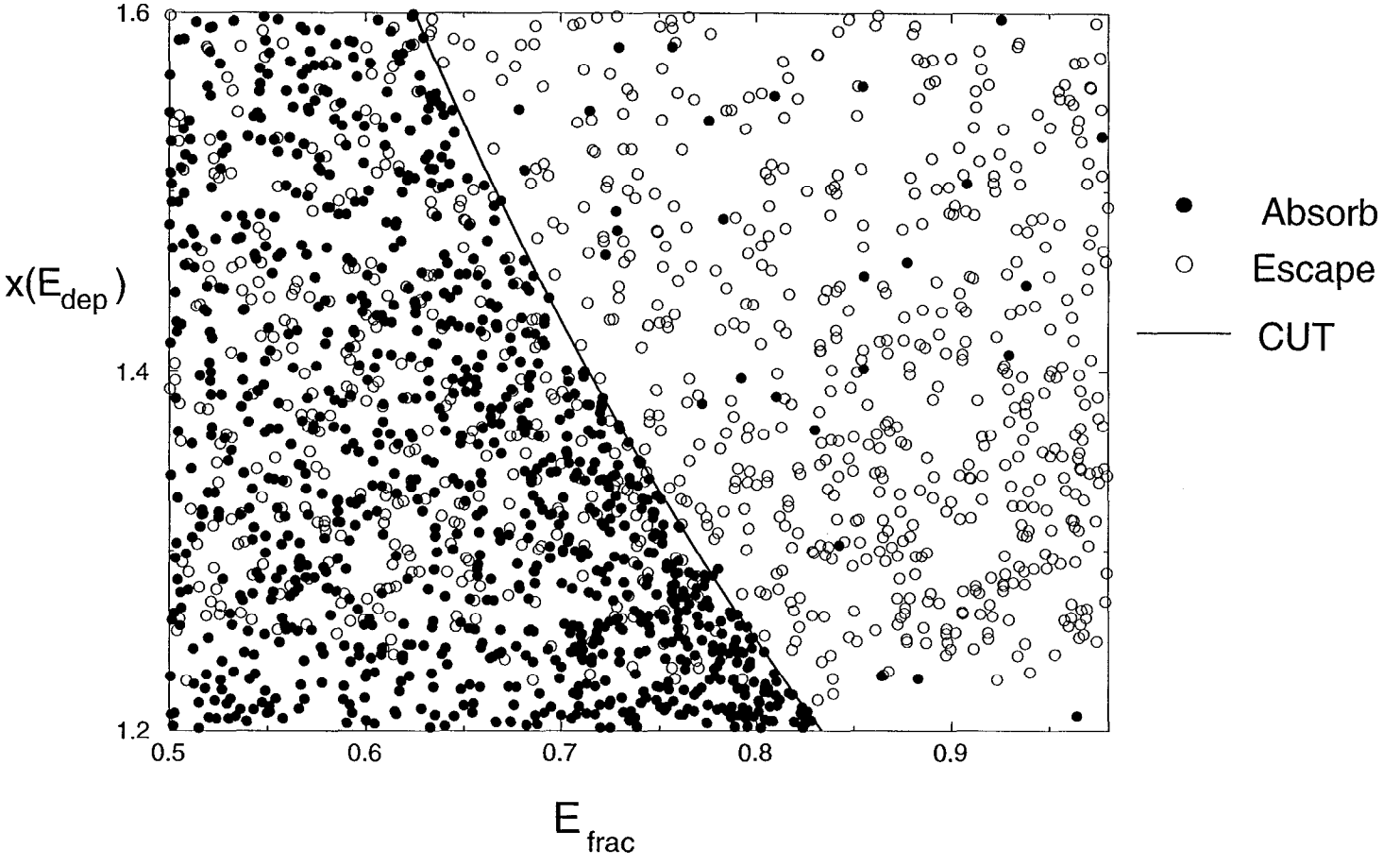

Figure 1

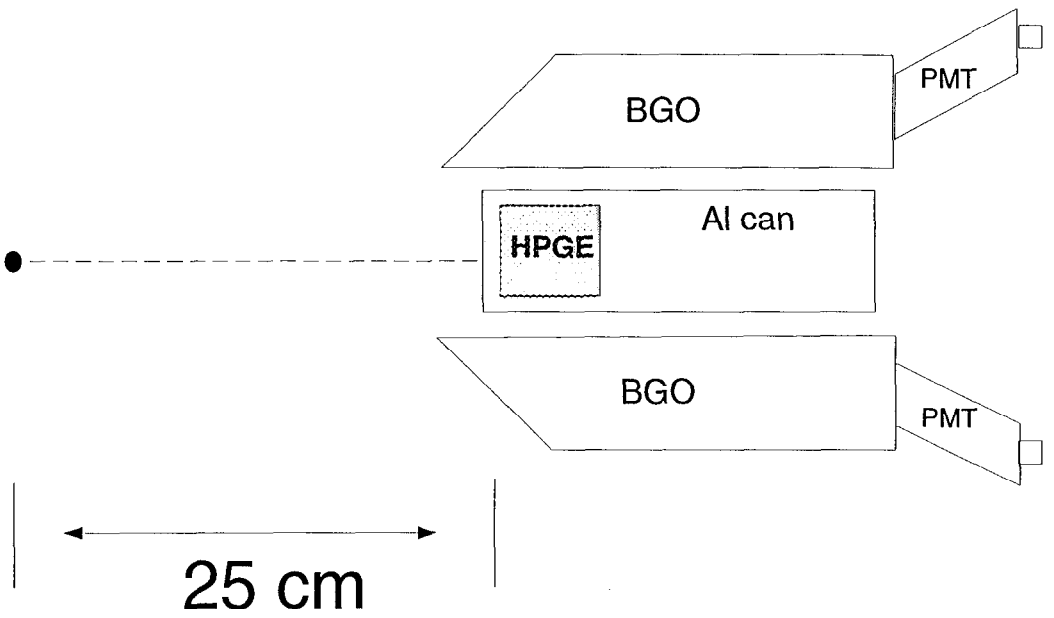

Figure 2

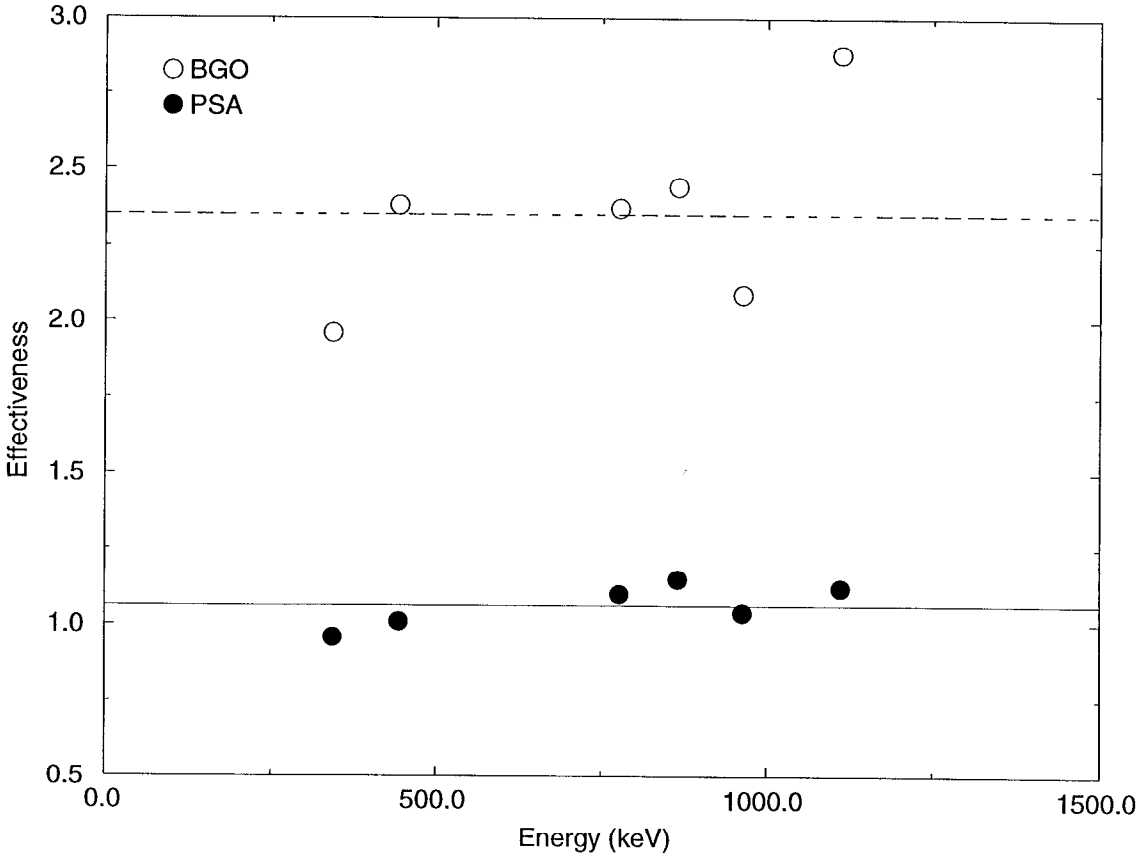
3.0
2.5
2.0
1.5
1.0
0.5
Effectiveness
BGO
PSA
0.0
500.0
1000.0
1500.0
Energy (keV)

Figure 3

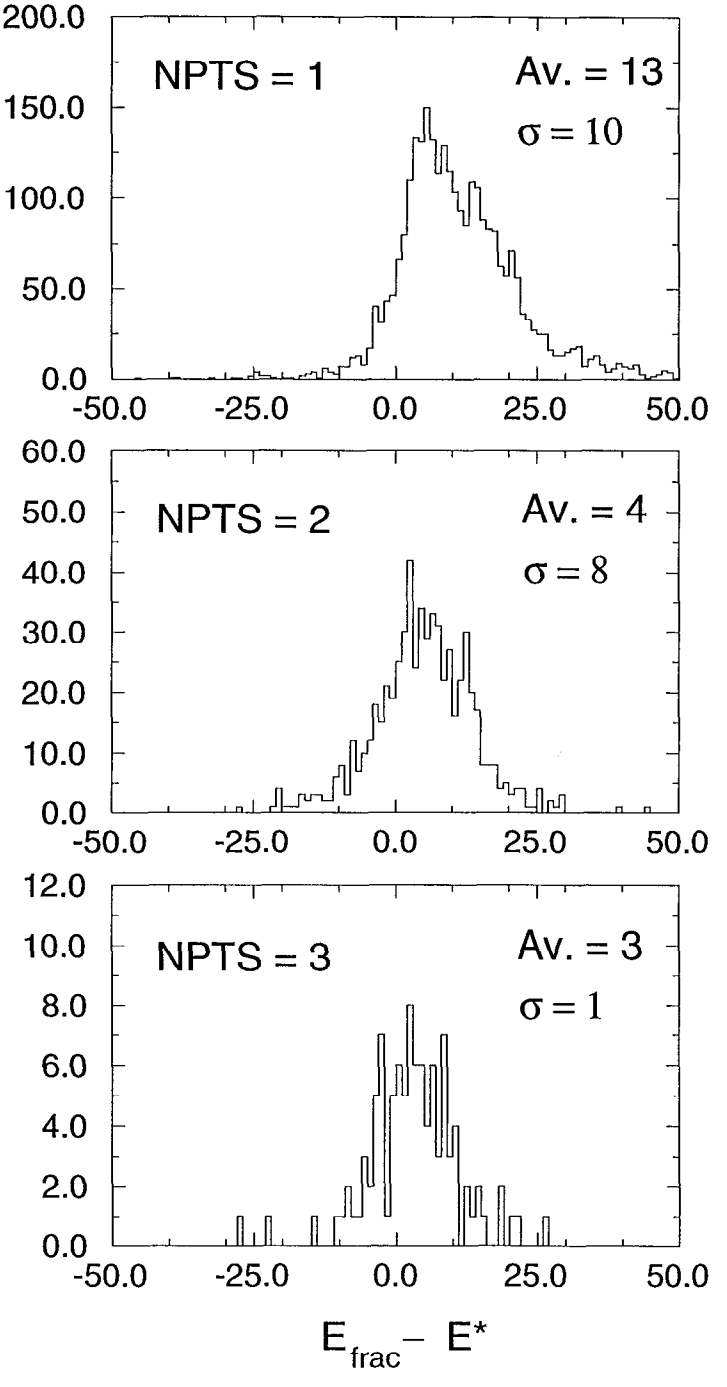
NPTS = 1
Av. = 13
σ = 10
NPTS = 2
Av. = 4
σ = 8
NPTS = 3
Av. = 3
σ = 1
200.0
150.0
100.0
50.0
0.0
60.0
50.0
40.0
30.0
20.0
10.0
12.0
10.0
8.0
6.0
4.0
2.0
-50.0
-25.0
0.0
25.0
50.0
E_frac − E*

Figure 4

Technical Information Department • **Lawrence Livermore National Laboratory**
University of California • Livermore, California 94551